



Flexible, Stretchable, and Rechargeable Fiber-Shaped Zinc–Air Battery Based on Cross-Stacked Carbon Nanotube Sheets

Yifan Xu, Ye Zhang, Ziyang Guo, Jing Ren, Yonggang Wang,* and Huisheng Peng*

Abstract: The fabrication of flexible, stretchable and rechargeable devices with a high energy density is critical for next-generation electronics. Herein, fiber-shaped Zn–air batteries, are realized for the first time by designing aligned, cross-stacked and porous carbon nanotube sheets simultaneously that behave as a gas diffusion layer, a catalyst layer, and a current collector. The combined remarkable electronic and mechanical properties of the aligned carbon nanotube sheets endow good electrochemical properties. They display excellent discharge and charge performances at a high current density of 2 A g^{-1} . They are also flexible and stretchable, which is particularly promising to power portable and wearable electronic devices.

Portable and wearable electronic devices with flexibility and stretchability have aroused increasing interests in recent years.^[1–6] There is a wide variety of applications for portable and wearable devices including flexible cell phones, human-like electronic skins, and intelligent bracelets. As a result, it is highly demanded to develop suitable power supply systems such as batteries and supercapacitors that share the properties of flexibility and stretchability.^[7–9] Among those energy devices, metal–air batteries have a relatively high capacity, and are more suitable for long-term power supply in wearable devices without charging. The zinc–air battery is a relatively mature technology, and its theoretical energy density reaches a value of 1086 W h kg^{-1} (including oxygen), which is approximately five times higher than that of the current lithium-ion battery.^[10] Meanwhile, Zn–air batteries also have the advantage of being low-cost and environmentally friendly, which shows broad perspectives for large manufacturing at low price.^[11]

However, conventional Zn–air batteries are typically flat and rigid, and thus cannot meet the requirements of portable and wearable devices.^[12–14] A Zn–air battery with cable-type

structure had been proposed to achieve the flexibility,^[15] but it was not stretchable and weavable. The miniaturized one-dimensional structure such as a fiber shape may provide an effective solution to produce flexible, stretchable and weavable Zn–air batteries.^[16] However, no Zn–air batteries with a fiber shape have been realized because of the high requirements for the air electrode. The air electrode is typically placed in the outermost layer of the Zn–air battery, and it can easily drop off when the fiber-shaped battery is bent and stretched. Compared to the previous work,^[17–21] a new type of air electrode with small thickness, light weight, good conductivity, and favorable mechanical properties, such as flexibility and stretchability, is desired. On the other hand, several attempts have been recently made to fabricate rechargeable Zn–air batteries,^[14, 20–23] but it also remains challenging to find appropriate air cathodes showing high performances.

Aligned carbon nanotube (CNT) materials such as sheets are promising materials that show high conductivities of 10^2 – 10^3 S cm^{-1} and high tensile strengths in the order of 10^2 – 10^3 MPa , and their remarkable electrical and mechanical properties can be easily extended to macroscopic scale for practical applications.^[24–28] The CNT sheets showed a porous structure by cross-stacking the aligned CNTs layer by layer, and the structures could be easily modified by varying the layer number and direction. Owing to the small thickness, light weight and flexibility, the material is promising to be used as an air electrode in Zn–air batteries which has not been reported yet.

Herein, a flexible, stretchable and rechargeable fiber-shaped Zn–air battery is produced from an air cathode that includes aligned and cross-stacked CNT sheet for the oxygen-reduction reaction (ORR) and a RuO_2 -based catalyst for the oxygen-evolution reaction (OER),^[29] a zinc spring anode and a free-standing hydrogel polymer electrolyte. O_2 is reduced to OH^- at the CNT sheet during the discharging procedure and OH^- is oxidized to O_2 during the charging procedure at the RuO_2 -based catalyst layer. Obviously, the CNT sheet layer also plays the role of a gas diffusion layer, adsorbing oxygen from the atmosphere, and a current collector to transport electrons. The CNT sheet-based air cathode provides the Zn–air battery with stable electrochemical properties under bending and stretching conditions, stable discharge at 10 A g^{-1} and high discharging/charging performances at a current density of 2 A g^{-1} .

The fabrication of the rechargeable fiber-shaped Zn–air battery is schematically shown in Figure 1. A zinc spring was first prepared by coiling a zinc wire onto a steel rod, followed by removing it from the rod (see Figure S1 in the Supporting Information). The zinc spring was then dipped into a hydrogel

[*] Y. Xu, Y. Zhang, J. Ren, Prof. H. Peng

State Key Laboratory of Molecular Engineering of Polymers, Department of Macromolecular Science, and Laboratory of Advanced Materials, Fudan University
Shanghai 200438 (China)
E-mail: penghs@fudan.edu.cn

Z. Guo, Prof. Y. Wang
Department of Chemistry and
Shanghai Key Laboratory of Molecular Catalysis and
Innovative Materials, Institute of New Energy, iChEM
(Collaborative Innovation Center of Chemistry for Energy Materials)
Fudan University, Shanghai 200438 (China)
E-mail: ygwang@fudan.edu.cn

Supporting information for this article is available on the WWW under <http://dx.doi.org/10.1002/anie.201508848>.

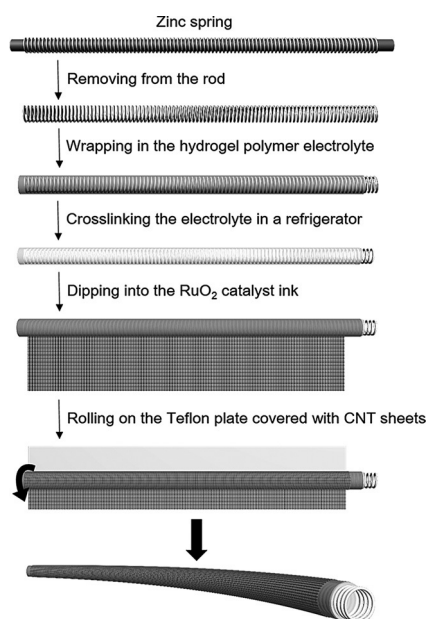


Figure 1. Schematic illustration to the fabrication of the fiber-shaped Zn-air battery.

polymer electrolyte solution and kept in a refrigerator for crosslinking of the electrolyte. The resulting string was further dipped into the catalyst ink of a RuO_2 ethanol suspension to form a catalyst layer on the surrounding surface of the hydrogel polymer electrolyte. A tetragonal phase of the RuO_2 hydrate was characterized by X-ray diffraction (Figure S2a) and the particle size was about 5 nm. Aligned CNT sheets were drawn from a spinnable CNT array^[30,31] and cross-stacked layer by layer onto a Teflon plate (Figure S3a). Finally, the modified zinc spring was rolled on the prepared Teflon plate covered with CNT sheets. The air electrode was porous with the CNTs remaining aligned (Figure S3b). As the CNT sheet air electrode also served as a current collector and a gas diffusion layer, no binder or additional conductive materials were required.

The hydrogel polymer electrolyte was composed of 8.3 wt % poly(vinyl alcohol) (PVA), 0.83 wt % poly(ethylene oxide) (PEO), and 8.3 wt % KOH. PEO was added to improve the mechanical properties of the electrolyte. The frozen preparation of the hydrogel polymer for KOH-based electrolyte displayed better mechanical properties and ionic conductivities compared to the other polymer electrolyte.^[32,33] The cross-linked electrolyte was free-standing, flexible and stretchable (with a maximal strain of 300%), and showed high ionic conductivity of 0.3 Scm^{-1} with 8.3 wt % KOH (Figure S4), which was close to the KOH water solution with the same concentration.

The structures and materials of the air electrode are crucial for the electrochemical performances of Zn-air batteries. They should be able to catalyze the ORR and OER and support the oxygen diffusion into the inner layer of the cathode. A flexible and thin CNT sheet air electrode was prepared to achieve both high porosity for gas diffusion and good contact with the hydrogel polymer electrolyte to realize the flexibility and stretchability of Zn-air battery. To inves-

tigate the structure effects of air cathodes on the electrochemical performance, air electrodes with different angles between two neighboring CNT sheets were compared. Figure 2a–d displays typical scanning electron microscopy (SEM) images of CNT sheet electrodes with increasing crossing angles of 0, 30, 60, and 90°. The CNTs remained highly aligned in the air electrode, and the aligned CNTs formed porous frameworks (Figures S5–8), which made it possible that oxygen rapidly diffused into the inner space of the air cathode.

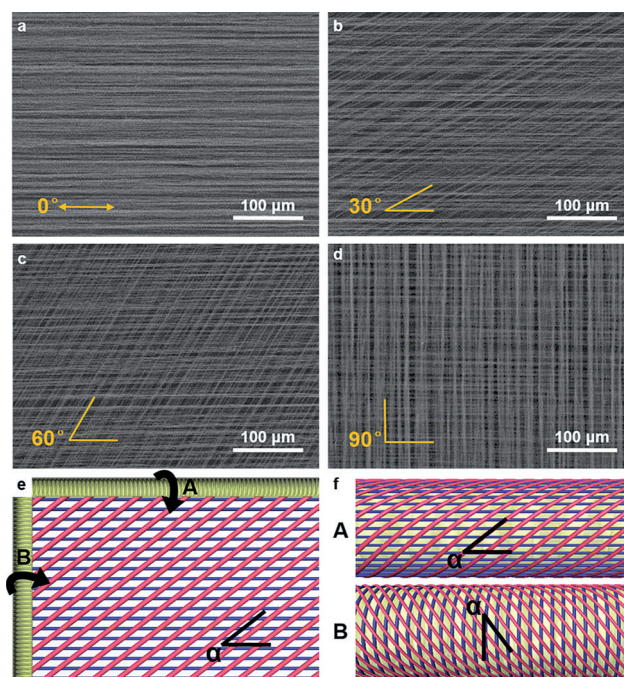


Figure 2. Structure characterizations of CNT sheet air electrodes. a–d) SEM images of CNT sheets with cross-stacking angles of 0, 30, 60, and 90°, respectively. e) Schematic illustration to methods A and B in rolling the stacked CNT sheet. f) Schematic illustration to the structure of the aligned CNT in the fiber-shaped Zn-air battery. The angle between the blue and the red aligned CNTs was labelled as α .

There are two methods to wrap the CNT sheet electrode (Figure 2e). The aligned CNTs are marked as blue and red lines in parallel and perpendicular directions, respectively. For method A, the modified Zn spring was rolled from the top to the bottom; for method B, the modified Zn spring was rolled from the left to the right. The structures of the resulting air cathodes are compared in Figure 2f. The blue lines form a cylinder parallel to the length direction while a number of rings are produced along the length direction for Methods A and B, respectively. For the air electrode, the neighboring CNT sheets were crossed with each other during the preparation, and the layer number (n) can be precisely controlled and calculated by $n = (l \times m) / C$, where l and m represent the rolled length of the Teflon plate and the number of stacked CNT sheet covered on the Teflon plate, respectively, and C is the circumference of the cross-section of the fiber-shaped Zn-air battery.

To investigate the influence of the air electrode, we compared the rate discharge performance of the fiber-shaped Zn–air batteries with different air electrode structures at various current densities (Figure 3a and b). Here all the Zn–air batteries were tested under ambient atmosphere condition. For method A, the discharge voltage plateaus decreased

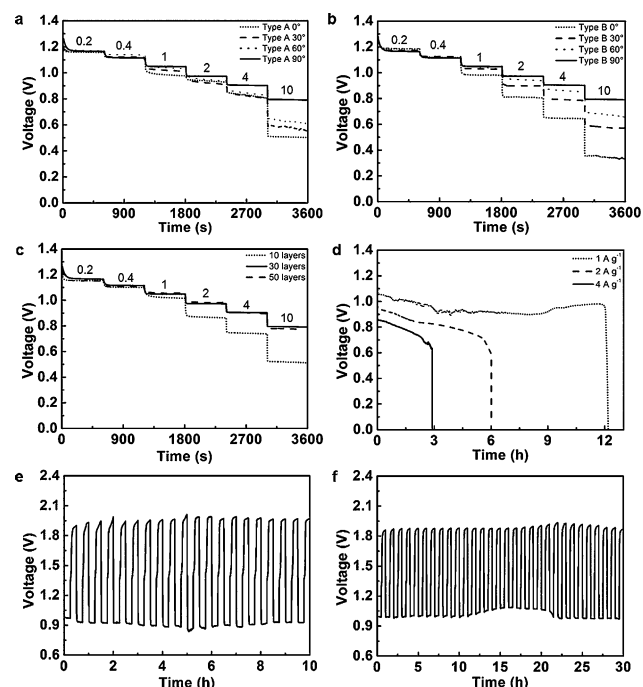


Figure 3. Electrochemical performance of the fiber-shaped Zn–air batteries. a,b) Rate discharge curves of the fiber-shaped Zn–air batteries with increasing cross-stacking angles from 0 to 90° at different current densities for methods A and B, respectively. The layer number of aligned CNT sheets in the air cathode was the 30 for both methods. c) Rate discharge curves of the fiber-shaped Zn–air batteries with increasing layer numbers of CNT sheets at different current densities at the same cross-stacking angle of 90°. The unit of the current density is Ag^{-1} . d) Galvanostatic discharge curves of the fiber-shaped Zn–air batteries. e,f) Discharge–charge curves of a fiber-shaped Zn–air battery at current densities of 2 and 1 Ag^{-1} , respectively. The length of the Zn–air batteries was 1 cm.

with increasing current densities when the angles between two neighboring CNT sheets were the same (Figure 3a). The discharge voltage plateaus were enhanced at higher angles between neighboring CNT sheets under discharging condition at the same current density, and this phenomenon was more obvious at high current densities. A discharge voltage plateau of 0.5 V was observed at an angle of 0°, and it reached 0.8 V at 90° at 10 Ag^{-1} (0.5 mA cm^{-2}). The air cathode tended to contract and the aligned CNTs tended to bundle together upon wrapping around the surface of the hydrogel electrolyte. The diffusion of oxygen became poorer in the air electrode and the discharge voltage dropped because of the low efficiency of the ORR. The above contractions would be decreased with increasing stacking angles as the aligned CNTs can be more effectively restricted by the neighboring CNTs. The contraction may be reduced to a minimum if the

neighboring CNT sheets were orthogonal to each other, producing the highest discharge voltage plateau. The fiber-shaped Zn–air battery produced using Method B showed this behavior (Figure 3b). The discharge rate performance of batteries produced using method A was better than for method B at 0° possibly due to a lower resistance. The aligned CNTs were parallel to the length direction of the fiber-shaped Zn–air battery in method A (Figure 2f), providing a better electron transport along the fiber-shaped battery. However, with the increasing angles between two neighboring CNT sheets, the angles started to dominate the Zn–air battery in performance rather than the resistance. Consequently, improved rate discharge performances were observed for method B. The discharge performances of the fiber-shaped batteries were compared for methods A and B under external forces such as stretching and bending, and a more stable performance was observed for method A (Figure S9). The two methods result in the same and best rate discharge property at 90°.

The aligned structure of the CNTs was important for the electrochemical performance of the fiber-shaped Zn–air battery. For comparison, the fiber-shaped Zn–air battery obtained from the randomly dispersed CNT film air cathode was also compared under the same conditions (Figure S10). Obviously, the randomly dispersed CNT film produced much poorer rate discharge properties, and the resulting fiber-shaped Zn–air battery cannot even be discharged at a relatively high current density of 10 Ag^{-1} .

The layer number of CNT sheets was also important for the battery performance. The rate discharge voltage remained almost unchanged for a layer number reaching 30 or more (Figure 3c). Certain layered CNT sheets were needed for the air cathode to adsorb and diffuse oxygen from the atmosphere for the ORR. Therefore, the fiber-shaped Zn–air batteries with 30 layers of CNT sheets, a cross-stacking angle of 90° and a length of 1 cm had been studied unless specified otherwise. The open-circuit potential of the fiber-shaped Zn–air battery was 1.29 V. Galvanostatic discharge measurements were conducted at different current densities to study the stability during the discharging process (Figure 3d). The duration time linearly decreased with increasing current density, showing approximately the same utilization of Zn. The end of discharge is probably caused by the insufficient electrochemical reaction inside the zinc spring.^[23] The energy and power densities of the fiber-shaped Zn–air battery were calculated as 6 Ah L^{-1} and 5.7 Wh L^{-1} , respectively.

This fiber-shaped Zn–air battery was rechargeable, as evidenced by discharging/charging at 2 and 1 Ag^{-1} at discharging voltages of 0.9 and 1.0 V (Figure 3e and f). Specifically, the discharging current density reached 1 Ag^{-1} at the voltage plateau of 1.0 V and was maintained for 30 discharge/charge cycles. The decreased potential polarizations at 6 h in Figure 3e and 15 h in Figure 3f may be explained by the evaporation of water in the hydrogel electrolyte which leads to a shape shrinkage with a structure change of the air electrode.^[32] The fully discharged battery could be charged back with a decrease of about 14% of the discharging voltage (Figure S11). Here RuO_2 hydrate was used as an OER catalyst (Figure S12) to catalyze the OER

during charging of the Zn–air battery, and the CNT sheet was used as an ORR catalyst layer. To clarify the function of the RuO₂ catalyst layer, fiber-shaped Zn–air batteries without dipping into RuO₂ catalyst ink were also fabricated and compared. Without the RuO₂ catalyst layer, the battery was not rechargeable, but its discharge performance was almost unaffected (Figure S13).

The fiber shape provided the Zn–air battery with flexibility and stretchability. A fiber-shaped Zn–air battery was bent to 30, 60, 90, 120, and 150° without obvious damage in structure (Figure 4a). Figure 4b further compares the dis-

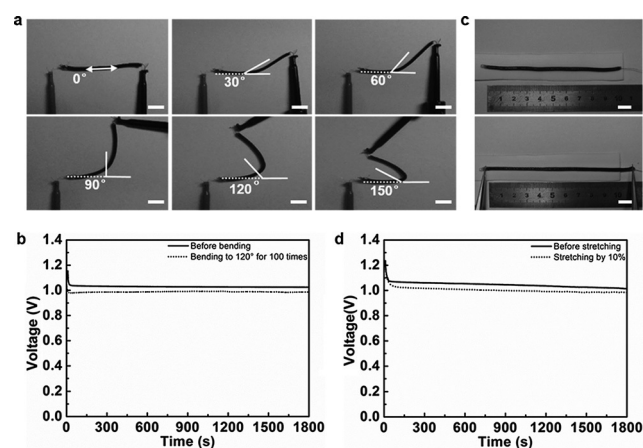


Figure 4. Characterization of the flexibility and stretchability of the fiber-shaped Zn–air batteries. a) Photographs of a fiber-shaped Zn–air battery bent to increasing angles; scale bar: 1 cm. b) Discharge curves of the fiber-shaped Zn–air battery with a length of 5 cm at a current density of 1 A g⁻¹ before and after bending to 120° for 100 cycles. c) Photographs of a fiber-shaped Zn–air battery before and after stretching by 10%, scale bar: 1 cm. d) Discharge curves of the fiber-shaped Zn–air battery with a length of 10 cm at a current density of 1 A g⁻¹ before and after stretching by 10%.

charge performance before and after bending (bent to 120° for 100 cycles). The discharge voltage remained almost unchanged at a current density of 1 A g⁻¹. The fiber-shaped Zn–air battery could also be stretched to a certain extent without breaking, for example, an elongation of 10% was made for a fiber-shaped Zn–air battery with a cross-stacking angle of 80° (Figure 4c). A quantitative study on the discharge voltage also verified the stable performance under stretching conditions (Figure 4d).

The remarkable electrochemical and mechanical performance may be explained by the following facts. First, the aligned, cross-stacked and porous CNT sheets with excellent electronic properties enable discharging/charging at a high current density. Second, all components were flexible and stretchable, which provides the battery with flexibility and stretchability. Third, the solid-state hydrogel polymer electrolyte served as a separator to prevent short circuits and leakages of electrolyte during stretching and bending.

In summary, to the best of our knowledge, a flexible, stretchable and rechargeable fiber-shaped Zn–air battery has been developed by using aligned CNT sheets for the air cathode and designing a spring structure. The battery can be

discharged/charged at 1 V at a high current density of 1 A g⁻¹ and is promising to power various miniaturized and wearable electronic devices.

Experimental Section

1 g PVA powder (MW 195 000, Aladdin) and 0.1 g PEO powder (MW 100 000, Alfa Aesar) were dissolved in 10 mL deionized water at 95 °C under magnetic stirring for about 2 h. Then 1 mL of 18 M KOH solution was added and the electrolyte solution was kept stirring at 95 °C for about 40 min. A zinc wire (250 μm in diameter) as the anode was wound onto a stainless steel rod with a pitch of 400 μm to form a spring. Then the rod was removed and the zinc spring was placed in a PET tube template (3.5 mm in diameter). The tube template was filled with the hydrogel polymer electrolyte solution. After it was kept in a refrigerator at –20 °C for 2 h to crosslink the electrolyte solution, the temperature was increased to 0 °C for 4 h to further enhance the crosslinking degree. The resulting spring was dipped into the RuO₂ catalyst ink, which was prepared by ultrasonically dispersing 80 mg RuO₂ hydrate in 20 mL ethanol to form the RuO₂ catalyst layer. It was finally rolled on the Teflon plate covered with the aligned and cross-stacked CNT sheets. Here the aligned CNT sheets were dry-drawn from a spinnable CNT array that was synthesized by chemical vapor deposition.^[31] The mass of the air electrode was calculated by the density of the CNT sheet. In the case of the randomly dispersed CNT layer, the same weight was used for the comparing study. A stainless steel wire was tied to the air electrode of the Zn–Air battery for electrochemical analysis.

Acknowledgements

This work was supported by MOST (grant number 2011CB932503), NSFC (grant number 21225417), STCSM (grant number 15XD1500400), the Fok Ying Tong Education Foundation, the Program for Special Appointments of Professors at Shanghai Institutions of Higher Learning, and the Program for Outstanding Young Scholars from the Organization Department of the CPC Central Committee.

Keywords: carbon materials · electrodes · flexibility · nanotubes · zinc–air batteries

How to cite: *Angew. Chem. Int. Ed.* **2015**, *54*, 15390–15394
Angew. Chem. **2015**, *127*, 15610–15614

- [1] Z. Yang, J. Ren, Z. Zhang, X. Chen, G. Guan, L. Qiu, Y. Zhang, H. Peng, *Chem. Rev.* **2015**, *115*, 5159–5223.
- [2] C. Choi, J. A. Lee, A. Y. Choi, Y. T. Kim, X. Lepro, M. D. Lima, R. H. Baughman, S. J. Kim, *Adv. Mater.* **2014**, *26*, 2059–2065.
- [3] Y. Kim, J. Zhu, B. Yeom, M. Di Prima, X. Su, J. G. Kim, S. J. Yoo, C. Uher, N. A. Kotov, *Nature* **2013**, *500*, 59–63.
- [4] G. S. Jeong, D. H. Baek, H. C. Jung, J. H. Song, J. H. Moon, S. W. Hong, I. Y. Kim, S. H. Lee, *Nat. Commun.* **2012**, *3*, 977.
- [5] T. Yamada, Y. Hayamizu, Y. Yamamoto, Y. Yomogida, A. Izadi-Najafabadi, D. N. Futaba, K. Hata, *Nat. Nanotechnol.* **2011**, *6*, 296–301.
- [6] B. Y. Ahn, E. B. Duoss, M. J. Motala, X. Guo, S. I. Park, Y. Xiong, J. Yoon, R. G. Nuzzo, J. A. Rogers, J. A. Lewis, *Science* **2009**, *323*, 1590–1593.
- [7] Y. Meng, Y. Zhao, C. Hu, H. Cheng, Y. Hu, Z. Zhang, G. Shi, L. Qu, *Adv. Mater.* **2013**, *25*, 2326–2331.
- [8] Z. S. Wu, Z. Liu, K. Parvez, X. Feng, K. Mullen, *Adv. Mater.* **2015**, *27*, 3669–3675.

- [9] K. H. Choi, S. J. Cho, S. H. Kim, Y. H. Kwon, J. Y. Kim, S. Y. Lee, *Adv. Funct. Mater.* **2014**, *24*, 44–52.
- [10] Y. Li, H. Dai, *Chem. Soc. Rev.* **2014**, *43*, 5257–5275.
- [11] Z. L. Wang, D. Xu, J. J. Xu, X. B. Zhang, *Chem. Soc. Rev.* **2014**, *43*, 7746–7786.
- [12] P. C. Li, C. C. Hu, T. C. Lee, W. S. Chang, T. H. Wang, *J. Power Sources* **2014**, *269*, 88–97.
- [13] S. Zhu, Z. Chen, B. Li, D. Higgins, H. Wang, H. Li, Z. W. Chen, *Electrochim. Acta* **2011**, *56*, 5080–5084.
- [14] J. Zhang, Z. Zhao, Z. Xia, L. Dai, *Nat. Nanotechnol.* **2015**, *10*, 444–452.
- [15] J. Park, M. Park, G. Nam, J.-s. Lee, J. Cho, *Adv. Mater.* **2015**, *27*, 1396–1401.
- [16] Y. Liang, Z. Wang, J. Huang, H. Cheng, F. Zhao, Y. Hu, L. Jiang, L. Qu, *J. Mater. Chem. A* **2015**, *3*, 2547–2551.
- [17] H. D. Lim, K. Y. Park, H. Song, E. Y. Jang, H. Gwon, J. Kim, Y. H. Kim, M. D. Lima, R. O. Robles, X. Lepro, R. H. Baughman, K. Kang, *Adv. Mater.* **2013**, *25*, 1348–1352.
- [18] H. D. Lim, H. Song, J. Kim, H. Gwon, Y. Bae, K. Y. Park, J. Hong, H. Kim, T. Kim, Y. H. Kim, X. Lepro, R. Ovalle-Robles, R. H. Baughman, K. Kang, *Angew. Chem. Int. Ed.* **2014**, *53*, 3926–3931; *Angew. Chem.* **2014**, *126*, 4007–4012.
- [19] Z. S. Wu, S. Yang, Y. Sum, K. Parvez, X. Feng, K. Mullen, *J. Am. Chem. Soc.* **2012**, *134*, 9082–9085.
- [20] T. Y. Ma, J. Ran, S. Dai, M. Jaroniec, S. Z. Qiao, *Angew. Chem. Int. Ed.* **2015**, *54*, 4646–4650; *Angew. Chem.* **2015**, *127*, 4729–4733.
- [21] D. U. Lee, J. Y. Choi, K. Feng, H. W. Park, Z. Chen, *Adv. Energy Mater.* **2014**, *4*, 1301389.
- [22] Y. Li, M. Gong, Y. Liang, J. Feng, J. E. Kim, H. Wang, G. Hong, B. Zhang, H. Dai, *Nat. Commun.* **2013**, *4*, 1805.
- [23] J. Fu, D. U. Lee, F. M. Hassan, L. Yang, Z. Bai, M. G. Park, Z. Chen, *Adv. Mater.* **2015**, DOI: 10.1002/adma.201502853.
- [24] S. Wang, E. Iyyamperumal, A. Roy, Y. Xue, D. Yu, L. Dai, *Angew. Chem. Int. Ed.* **2011**, *50*, 11756–11760; *Angew. Chem.* **2011**, *123*, 11960–11964.
- [25] S. Iijima, *Nature* **1991**, *354*, 56–58.
- [26] J. Nardelli, T. J. Gibson, C. Vesque, P. Charnay, *Nature* **1991**, *349*, 175–178.
- [27] M. F. L. de Volder, S. H. Tawfick, R. H. Baughman, A. J. Hart, *Science* **2013**, *339*, 535–539.
- [28] W. Xiong, F. Du, Y. Liu, A. Perez Jr., M. Supp, T. S. Ramakrishnan, L. Dai, L. Jiang, *J. Am. Chem. Soc.* **2010**, *132*, 15839–15841.
- [29] Y. Fang, Z. Liu, *J. Am. Chem. Soc.* **2010**, *132*, 18214–18222.
- [30] M. Zhang, K. R. Atkinson, R. H. Baughman, *Science* **2004**, *306*, 1358–1361.
- [31] T. Chen, L. Qiu, Z. Yang, Z. Cai, J. Ren, H. Li, H. Lin, X. Sun, H. Peng, *Angew. Chem. Int. Ed.* **2012**, *51*, 11977–11980; *Angew. Chem.* **2012**, *124*, 12143–12146.
- [32] A. Lewandowski, K. Skorupska, J. Malinska, *Solid State Ionics* **2000**, *133*, 265–271.
- [33] C. C. Yang, S. J. Lin, *J. Power Sources* **2002**, *112*, 497–503.

Received: September 21, 2015

Revised: October 4, 2015

Published online: October 30, 2015